

SENSOR STUDIES FOR DC CURRENT TRANSFORMER APPLICATION

E. Soliman, K. Hofmann, Technische Universität Darmstadt, Darmstadt, Germany
H. Reeg, M. Schwickert, GSI Helmholtzzentrum für Schwerionenforschung GmbH, Darmstadt, Germany

Abstract

DC Current Transformers (DCCTs) are known since decades as non-intercepting standard tools for online beam current measurement in synchrotrons and storage rings. In general, the measurement principle of commonly used DCCTs is to introduce a modulating AC signal for a pair of ferromagnetic toroid. A passing DC ion beam leads to an asymmetric shift of the hysteresis curves of the toroid pair. However, a drawback for this measurement principle is found at certain revolution frequencies in ring accelerators, when interference caused by the modulating frequency and its harmonics leads to inaccurate readings by the DCCT. Recent developments of magnetic field sensors allow for new approaches towards a DCCT design without using the modulation principle. This paper shows a review of different kinds of usable magnetic sensors, their characteristics and how they could be used in novel DCCT instruments.

INTRODUCTION

Commonly, DCCTs are the main tool in synchrotrons and storage rings for online monitoring of DC beam currents. The SIS100 heavy ion synchrotron will be the central machine of the FAIR (Facility for Antiproton and Ion Research) accelerator complex currently under construction at GSI. Beam operation at SIS100 requires a novel DCCT device with large dynamic range and high accuracy [1]. Currently a Novel DCCT (NDCCT) based on modern magnetic field sensors is under development at GSI. Main motivation for this research project is to investigate different commercially available magnetic field sensors with regard to their applicability for reliable beam current measurements with the goal to simplify the device as compared to the conventional DCCT setup.

Figure 1 presents the schematic of a conventional DCCT sensor, consisting of two symmetrical toroid and modulator/demodulator circuit. In this setup the modulator circuit drives the two cores to magnetic saturation with a 180° phase shift. In case a DC current passes through the two cores the magnetic flux density generated in the cores is shifted asymmetrically. The sum of the total magnetic flux of the two cores is proportional to the DC current amplitude. A feedback circuit is used to compensate the change in the magnetic flux inside the

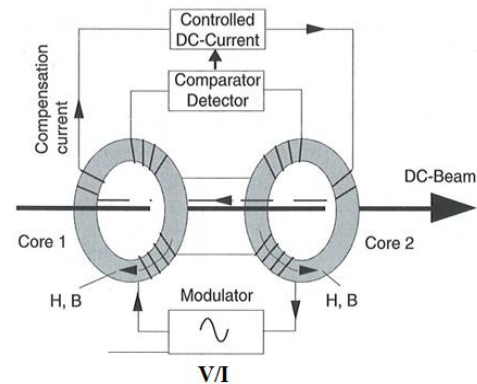


Figure 1: Conventional DCCT Block diagram [2].

cores to reach zero flux. The output current signal of the feedback circuit is a direct measure for the DC current passing the DCCT [3].

Besides many quality characteristics, a major disadvantage of this design is the fact that for precise beam current measurements the magnetic properties of the two ring cores must be perfectly matched, which requires an intricate manufacturing process. A second drawback of this setup, especially for the usage at SIS100, is the fact that the modulation frequency is 20 kHz; when the beam's basic revolution frequency or harmonics are the same as the even harmonics of the modulating frequency interference occurs. Therefore, the current measurement of a conventional DCCT becomes erroneous without notification to the user.

Thus, the requirement for a simpler DCCT assembly with a single core and without using the modulation technique came up. The principle for current sensing in the NDCCT is using commercially available integrated circuit magnetic field sensors. The sensitivity of modern sensors is sufficient to directly measure the magnetic field as generated by the DC ion beam current, without the need of using the modulation technique.

In Fig.2 a schematic view of an open loop NDCCT is depicted. The NDCCT consists of a high permeability slotted flux concentrator which allows for easy installation of the setup around the ceramic gap without breaking the vacuum. The magnetic sensor is placed inside the air gap of the flux concentrator.

*Work supported by BMBF; Project. No.: 05P12RDRBG between GSI and TU Darmstadt

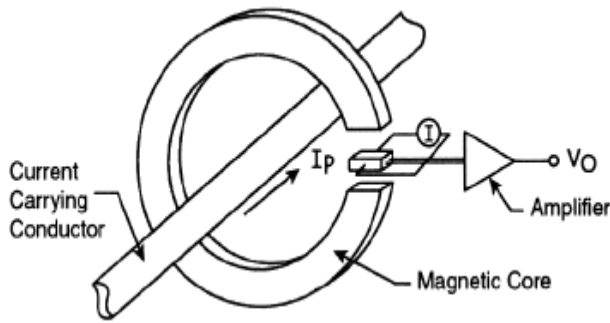


Figure 2: Schematic of NDCCT [4].

The magnetic sensor output voltage is proportional to the magnetic field inside the air gap. Additionally, an amplifier is implemented on the sensor PCB to amplify the output signal to increase sensitivity. Different types of commercially available magnetic sensors ICs were tested for magnetic field detection.

A conventional Hall sensor does not meet the NDCCT requirements due to a relatively low sensitivity and high power consumption. Today, different types of magneto-resistance (MR) sensors are commercially available. They have higher sensitivity and consume lower power than Hall sensors. In addition they are available in different IC packages like SOP8 and DFN8 ones, even as bondable dies. In the following we present an overview of MR sensor types and discuss their applicability for the NDCCT design.

MAGNETORESISTANCE SENSORS

MR sensors are based on a quantum mechanical magnetoresistance effect. The MR effect refers to the change of the material’s electrical resistivity in response to a change of an external magnetic field. This change in the material’s resistivity was found to be about 5% percent maximum in ferromagnetic materials, but could be enhanced significantly in thin film multilayer structures of alternating ferromagnetic/non-magnetic materials.

- There are three main types of MR sensors:
- Anisotropic Magneto-Resistance (AMR),
 - Giant Magneto-Resistance (GMR)
 - Tunnelling Magneto-Resistance (TMR).

The three sensor types vary in their multilayer structure. The functional structure is identical for all MR sensors. Four thin film resistors form a Wheatstone bridge. If an external magnetic field is applied the resistor’s value changes and consequently the output voltage of the bridge changes as well.

In Fig.3 and Fig.4 the physical and functional structures of GMR and TMR sensors are given. The difference between GMR and TMR is that the GMR has two shielded resistors in the bridge and this causes unipolar output voltage in contrast to the bipolar output voltage of the TMR.

The MR sensors are available from different companies. AMR IC sensors are produced by Honeywell

Company [7], GMR by NVE Company [5] and TMR by Dowaytech Company [6]. All sensors are available in SOP8 packages, except for TMR which is also available in DFN8 package.

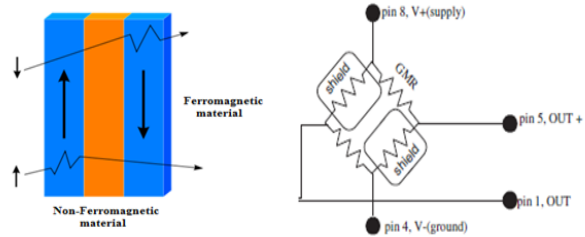


Figure 3: GMR Physical and Functional Structures [5].

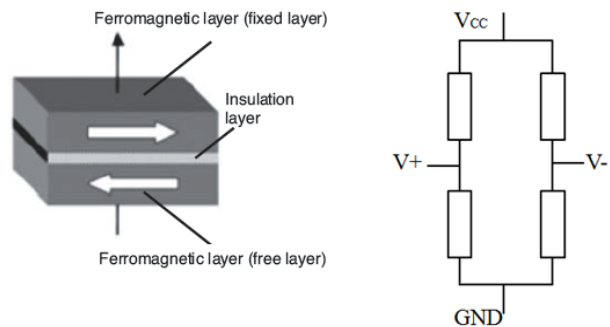


Figure 4: TMR Physical and Functional Structures [6].

MR SENSORS STUDY FOR NDCCT

In an earlier research project at GSI on the NDCCT a comparison between different commercial types of AMR and GMR sensors had been performed [8]. The result was that the GMR sensor from NVE Company [5] has a higher sensitivity to the magnetic field inside the air gap as compared to AMR. In addition, different types of GMR sensors from NVE were investigated and the best performance was reported for the AA002 type [8]. At the time of the study the TMR sensors were not yet available so the study didn’t include them

To continue investigating the MR sensors two PCBs were fabricated to compare the performance of GMR and TMR sensors. Fig.5 and Fig.6 show the PCBs for GMR and TMR, respectively. The PCB contains a MR sensor and an instrumentation amplifier to amplify the output signal of the voltage bridge generated by the sensor. The amplifier gain was set to 10.

The GMR sensor is from NVE (type AA002), and the TMR sensors are available in two types, MMLH45F and MMLP57F, each with a different sensitivity. As stated in the TMR datasheets; the sensitivity of MMLH45F and MMLP57F is 12mV/V/Oe and 4.9mV/V/Oe. As for the GMR, the AA002 sensitivity is 3mV/V/Oe. To calculate the magnetic flux density inside the air gap of the flux

concentrator the following formula was derived:

$$B_{gap} \approx \mu_o \frac{I}{d} \tag{1}$$

Where B_{gap} is the magnetic field inside the air gap in Tesla, μ_o is the vacuum permeability in T.m/A, I is the beam current and d is the air gap width in m, ($\mu_r \gg 1$).

As a first step towards characterising the PCBs of GMR and TMR sensors, a test of the sensors functionality using a permanent magnet was done. The value of the magnetic field at the sensor was measured using a Hall probe (Steingröver FH48). The DC output voltage of the PCB is measured versus the magnetic field by varying the distance between the permanent magnet and the magnetic sensor PCB. The results for the GMR and TMR sensors types are shown in Fig.7, 8 and 9, respectively. The measurement results are fitted linearly for positive and negative values separately. The standard error between the measurement points and the fitted curve is given as bar data points with scale on the right Y-axis of the graph.



Figure 5: GMR Test PCB.

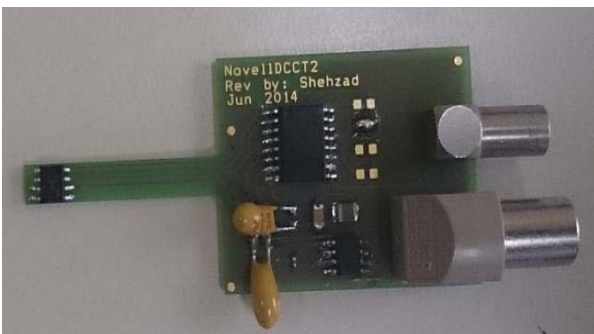


Figure 6: TMR Test PCB.

The results showed that both TMR sensors have bipolar transfer characteristics as expected, in contrast to the GMR sensor. TMR sensors have higher sensitivity compared to the GMR. Also with the use of the op-amp both types of TMR sensors display a comparable sensitivity.

If equation (1) were used to calculate the DC current needed to have a magnetic field value of $\pm 1.25\text{mT}$ in a 10mm air gap width, then the current value will be $\pm 10\text{A}$.

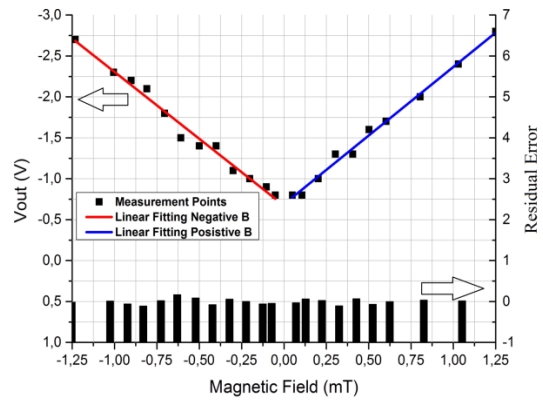


Figure 7: GMR PCB Output Voltage.

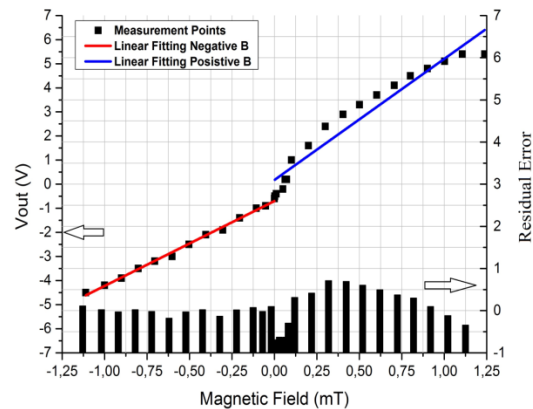


Figure 8: TMR MMLP57FP PCB Output Voltage.

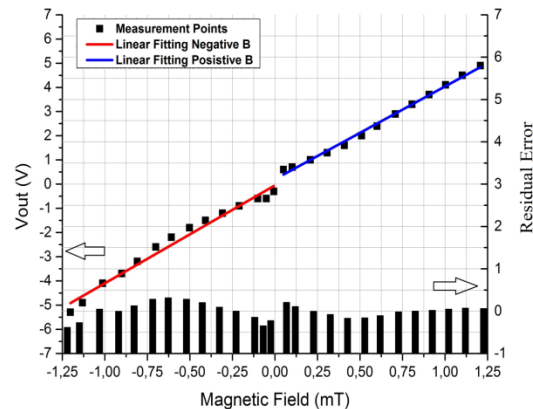


Figure 9: TMR MMLH45F PCB output Voltage.

Table 1 contains the slope of the measurement fitting curves and standard error present in Figs. 7, 8 and 9. It shows the sensitivity of the PCB's output voltage toward the magnetic field variation.

Table 1: Sensitivity of PCB Output Voltage to Magnetic Field

Sensor	Negative B		Positive B	
	Slope (V/mT)	Error	Slope (V/mT)	Error
GMR AA002	1.671	0.0492	-1.633	0.0652
TMR MMLP57F	3.522	0.0661	5.025	0.3359
TMR MMLH45F	4.047	0.1697	3.837	0.0842

NDCCT DC WIRE TEST

A test setup has been prepared for the NDCCT. As shown in Fig.10 it consists of a ring core flux concentrator from VAC Company (Vitrovac ‘6025F’). The flux concentrator permeability is very high (above 100000) and the width of the air gap is 10 mm, the inner and outer diameter is 200 mm and 250 mm, respectively. A mechanical support was produced to hold the flux concentrator. In addition a soft iron box in Fig. 10 for shielding covers the whole NDCCT test setup. A DC current was generated in a conducting wire at the centre of the core. The wire was terminated with a 50Ω load. The purpose of the test was to measure the resolution of the NDCCT. An Agilent signal generator was used to generate the DC current. The values of the generated current are ±50mA and this will produce a magnetic field of ±0.0625mT inside a 10 mm air gap width.

The experimental result for the test setup using the two types of the TMR PCB is shown in Fig. 11 and 12 for the SOP8 MMLH45F and MMLP57F, respectively. The results shown in Fig. 11 and 12 are the output voltage of the PCB used to test the TMR sensors versus the input DC current generated in the wire at the centre of the flux concentrator. The corresponding magnetic flux density’s value in the ring core air gap is shown on the upper X-axis of the figure. The sensitivity of the NDCCT is given by the slope of the curves shown in Fig. 11 and 12. The sensitivity of the TMR MMLH45F and MMLP57F sensors PCB are 0.382 V/A and 0.189 V/A respectively.

As stated in this paper’s introduction, the TMR fabricating Company additionally offers another package than the regular SOP8 (MMLP57FP), that is to say the MMLP57F sensor in a DFN8 package (MMLP57FD). This new package has a width of only 3 mm, hence halving the air gap’s width to 5 mm. In Fig. 13 the two packages of the TMR sensor are shown (6 mm x 3 mm x 1.5 mm and 3 mm x 3 mm x 0.75 mm). A special PCB for the DFN8 package was fabricated at GSI to test the sensor response against DC input current variation. This PCB is shown in Fig. 14.



Figure 10: NDCCT Test Setup.

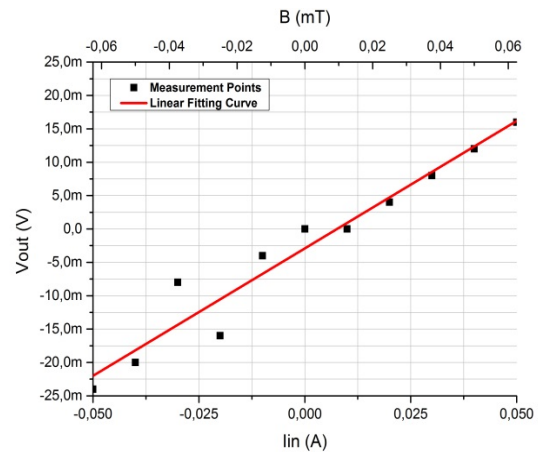


Figure 11: Output voltage of the DC wire test for TMR MMLH45F (Standard Error: 0.03102).

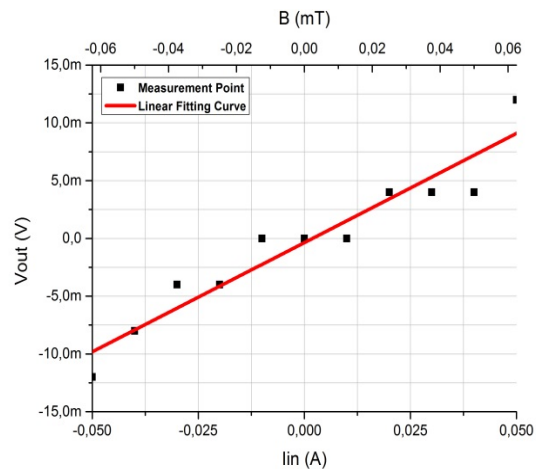


Figure 12: Output voltage of the DC wire test for TMR MMLP57FP (Standard Error: 0.01939).

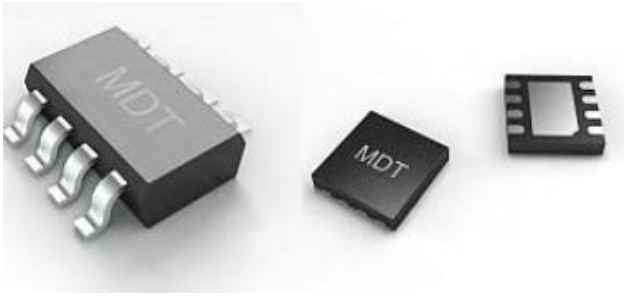


Figure 13: TMR MMLP57F packages [6].

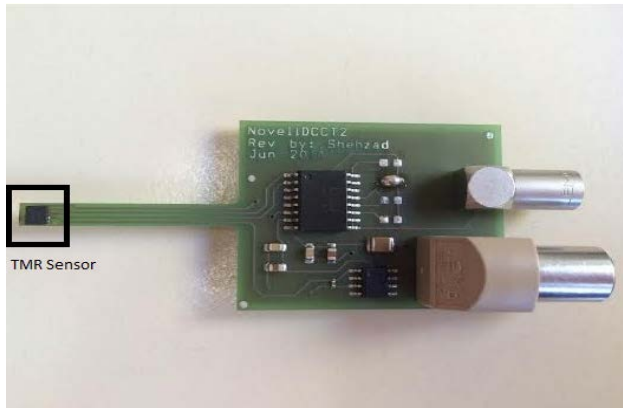


Figure 14: MMLP57FD customized PCB.

The DC wire test was done using the DFN8 package. The PCB width used for this sensor is reduced from 10mm to 5mm and thus the air gap size is halved. For example, $\pm 50\text{mA}$ DC current will generate $\pm 0.125\text{mT}$ in a 5 mm air gap width. The experimental result of the MMLP57FD TMR sensor is shown in Fig.15. The output voltage of the PCB is plotted versus the input current and the magnetic field generated in the air gap on the lower and upper X-axis, respectively. The sensitivity of the NDCCT setup is given by the slope of the curve, i.e. 0.416 V/A . The MMLP57FD sensor shows twice the sensitivity compared to the MMLP57FP sensor.

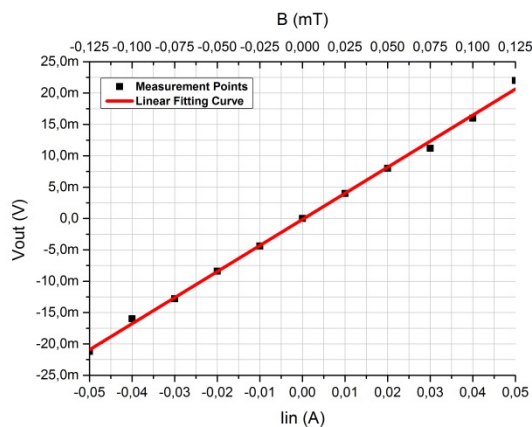


Figure 15: Output voltage of the DC wire test for MMLP57FD (Standard error: 0.00645).

CONCLUSION

A NDCCT based on the use of MR sensors is currently under development at GSI for the FAIR project. The NDCCT measures the DC current stored in the synchrotrons and storage rings by sensing the magnetic field generated by the ion beam current using MR sensors.

A comparative study of TMR and GMR sensors was performed to evaluate the advantages and disadvantages for the NDCCT design. As expected the TMR showed a bipolar transfer characteristics and higher sensitivity than the GMR sensor. Also different types of TMR sensors were examined to find the most sensitive type. The MMLH45F TMR sensor from Dawaytech Company is the most sensitive one according to the datasheets and the experimental results. A test setup for the NDCCT was built at GSI. The magnetic field generated by a DC current was measured using different TMR sensor types.

OUTLOOK

Future work for the NDCCT is to study the design for higher DC beam current values by using a power amplifier in the setup. The second step will be to add extra circuitry to measure the AC component of the NDCCT. A feedback system is foreseen to improve the device linearity and frequency response. Noise analysis and measurement is currently under investigation.

ACKNOWLEDGMENT

I would like to thank all my colleagues at GSI beam instrumentation department and at TU Darmstadt for their support during the test setup.

REFERENCES

- [1] M. Schwickert et al., "Beam Diagnostic for SIS100 at FAIR", DIPAC'11, May 2011, p. 41 (2011); <http://www.JACoW.org>
- [2] S. Zorzetti, "Digital Signal Processing and Generation for a DC Current Transformer for Particle Accelerators", BE/BI CERN.
- [3] P. Forck, "Lecture Notes on Beam Instrumentation and Diagnostics", Joint University Accelerator School, January – March 2013.
- [4] Bob Mammano, "Current Sensing Solutions for Power Supply Designers", Texas Instruments.
- [5] <http://www.nve.com/index.php>
- [6] <http://www.dawaytech.com/en/>
- [7] <http://sensing.honeywell.com/>
- [8] M. Häpe et al., "High Dynamic Magnetic Beam Current Measurements by Means of Optimised Magneto-resistance Sensor Engineering", DIPAC'05, May 2005, p. 102 (2005); <http://www.JACoW.org>